Impact of Myocardial Infarction Scar Size and Location on Left Ventricular Ejection Fraction

Jonathan Krauß, Tobias Gerach, Cristian Barrios Espinosa, Stephanie Appel, Axel Loewe

Karlsruhe Institute of Technology (KIT), Karlsruhe, Germany

Abstract

Coronary artery disease (CAD) can lead to myocardial scarring and impaired left ventricular ejection fraction (LVEF), a key parameter in clinical decision-making. This study investigates how scar size and location influence LVEF using electro-mechanical whole heart simulations.

We modeled scars resulting from occlusions in the left anterior descending artery (LAD), right coronary artery (RCA), and left circumflex artery (LCx), based on LGE-CMR statistics from single-vessel CAD patients. Simulations were performed on two heart anatomies, considering three scar sizes (6.5 %, 12.9 %, and 19.4 % of LV volume) and five locations per size and artery. In total, 92 electro-mechanical simulations were conducted.

LCx-related scars led to the most pronounced reductions in LVEF across both anatomies and all scar sizes (mean LVEF reductions at maximum scar size: LCx: 15.43 %, RCA: 11.05 %, LAD: 10.65 %). When analyzing LVEF against the total affected myocardial volume (scar + gray zone), we observed that the impact of LCx scars on LVEF remained greater than that of RCA and LAD scars.

Clinical studies showed that scar size is an independent predictor of ventricular arrhythmias, irrespective of LVEF. Combined with our finding that LVEF impairment depends on scar location, this suggests that decisions regarding ICD therapy should incorporate scar metrics rather than LV function alone.

1. Introduction

Coronary artery disease (CAD) can lead to the formation of scar tissue and in turn to reduced left ventricular ejection fraction (LVEF) [1]. LVEF plays an important role in clinical decision-making [2], e.g. for cardiac resynchronization therapy [3] and implantable cardioverter defibrillators (ICDs) [4]. However, while LVEF $\leq 35\,\%$ is strongly associated with all-cause and cardiac death, its prognostic value for sudden cardiac death (SCD) is weak compared to that of scar extent [5]. This highlights the need for a better understanding of the relationship between myocardial scar characteristics and functional impairment. In this study, we investigated whether the location of a scar impacts its effect on LVEF.

2. Material and methods

2.1. Study design

We performed electro-mechanical whole-heart simulations for three different scar regions in the left ventricle (LV) corresponding to occlusions of three different infarct related arteries (IRAs), namely left anterior descending artery (LAD), right coronary artery (RCA) and left circumflex artery (LCx). Scar size and IRA regions were based on the mean values $\pm$ 1 standard deviation of the manual assessment of left ventricle LGE-CMR data from 34 single-vessel CAD patients [6]. We examined scars of approximately $19.4\,\%$ (severe), $12.9\,\%$ (moderate) and $6.5\,\%$ (mild) of the LV myocardial volume. For each scar size and IRA, we simulated five possible locations on two different whole-heart geometries. The study design is shown in Figure 1. In total, we carried out 92 simulations (2 geometries $\times$ 3 scar regions $\times$ 3 scar sizes $\times$ 5 scar locations + 2 control simulations).

2.2. Simulation setup

This study is based on the electro-mechanical model of Gerach & Loewe [7]. We considered two different anatomies. Anatomy `Gerach` corresponds to the geometry used in [7], generated from MRI data of a 33-year old male healthy volunteer [8].

Anatomy `Rodero-01` corresponds to instance '01' from the virtual cohort of adult healthy hearts based on CT imaging published by Rodero et al. [9]. We computed atrial materials and fibers using *AugmentA* [10] and added a volumetric representation of the pericardium to the mechanics mesh in order to restrict the movement of the epicardial surface [11].

The gray zone separating scar and healthy myocardium had a width of $\approx 6\,\mathrm{mm}$. It was automatically gener-

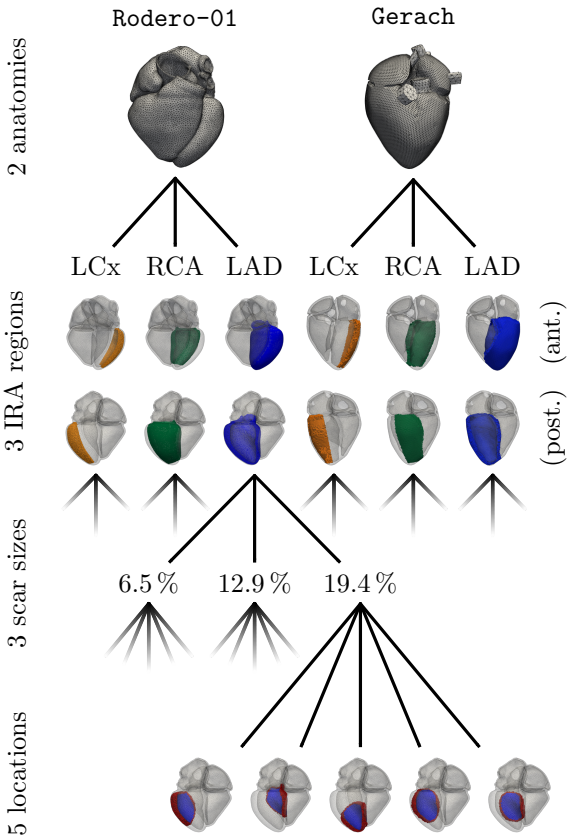

Figure 1. Study design consisting of 2 anatomies, 3 IRAs (and their corresponding potential scar regions taken from [6]), 3 scar sizes and 5 scar locations based on the potential scar regions of their respective IRA.

ated based on the scar geometry, leading to different total affected myocardial volumes (scar + gray zone) for the same scar size but different scar shapes. Ventricular cellular electrophysiology was described using the ten Tusscher et al. [12] model. Ion channel conductances were modified according to Salvador et al. [13]:

$$G_{\mathrm{Na}} = \left(0.38 + \frac{10}{9}\left(\eta - 0.1\right)\left(1 - 0.38\right)\right)\hat{G}_{\mathrm{Na}} \quad (1)$$

$$G_{\mathrm{CaL}} = \left(0.31 + \frac{10}{9}\left(\eta - 0.1\right)\left(1 - 0.31\right)\right)\hat{G}_{\mathrm{CaL}} \quad (2)$$

$$G_{\mathrm{Kr}} = \left(0.30 + \frac{10}{9}\left(\eta - 0.1\right)\left(1 - 0.30\right)\right)\hat{G}_{\mathrm{Kr}} \quad (3)$$

$$G_{\mathrm{Ks}} = \left(0.20 + \frac{10}{9}\left(\eta - 0.1\right)\left(1 - 0.20\right)\right)\hat{G}_{\mathrm{Ks}} \quad (4)$$

with G_X as the conductance for ion channel X and $\hat{G}_X$ as its healthy reference value. η is a parameter that allows for a linear interpolation between fully healthy case ($\eta = 1.0$) and gray zone ($\eta = 0.1$) modifications based on patch clamp recordings [14]. Scar tissue was modeled as electrically inactive. Additionally, electrical conductivities and mechanical stiffness were scaled in accordance with [13]:

$$\boldsymbol{D} = \eta\hat{\boldsymbol{D}} \quad (5)$$

$$C = \left(\eta + 4.56\left(1 - \eta\right)\right)\hat{C}. \quad (6)$$

$\hat{\boldsymbol{D}}$ and $\hat{C}$ are the diffusion tensor and mechanical stiffness for healthy myocardium. Corresponding values were taken from [7]. Following [13], η was set to be 1.0 for healthy tissue, 0.1 for the gray zone, and 0.0 for scar tissue. The remaining parameters, including atrial electrophysiology and mechanics as well as circulatory system model properties, were taken from [7].

Simulations were run for three heartbeats with a basic cycle length of 0.8 s ($\widehat{=}$75 bpm). Results are reported for the last cycle.

3. Results

Mean LVEFs for `Gerach` and `Rodero-01` are shown in Fig. 2 and Fig. 3, respectively. Occlusions from LCx scars led to the highest reduction in LVEF for each evaluated scar size and for both anatomies. For the `Gerach` anatomy, LVEF reduction was more prominent for RCA scars than for LAD scars. Severe scars led to mean EFs of 42.23 %, 41.01 % and 38.52 % for LAD, RCA and LCx scars, respectively (control: 51.47 %). For `Rodero-01` (see Fig. 3), LAD and RCA scars led to approximately the same mean LVEFs (mild: 56.33 % to 56.27 %, moderate: 52.33 % to 52.50 %). For the severe cases, mean LVEF results were 48.55 %, 48.97 % and 42.71 % for LAD, RCA and LCx scars, respectively (control: 60.61 %).

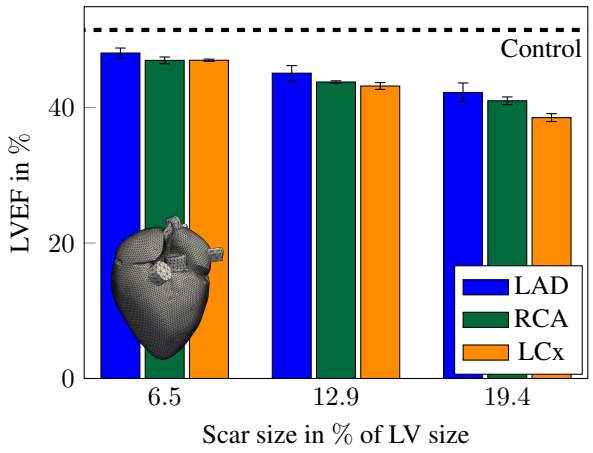

Figure 2. Mean ($n = 5$) LVEF for heart anatomy `Gerach` (bottom left) for scars from LAD (blue), RCA (green) and LCx (orange) occlusions. Dashed line represents control LVEF (no scar tissue) of 51.47 %.

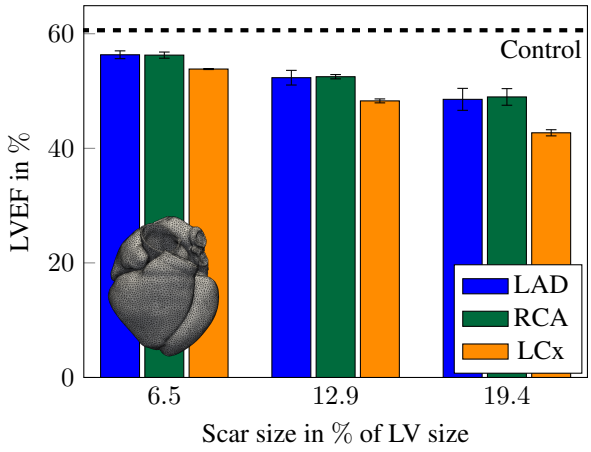

Figure 3. Mean ($n = 5$) LVEF for heart anatomy `Rodero-01` (bottom left) for scars from LAD (blue), RCA (green) and LCx (orange) occlusions. Dashed line represents control LVEF (no scar tissue) of 60.61 %.

Figure 4 presents ejection fraction outcomes across all `Rodero-01` simulations relative to the total affected myocardial volume (combined size of scar and gray zone). Regression lines for LAD and RCA scars are almost visually indistinguishable ($m_{\mathrm{LAD}} = -0.291\,\%\,\mathrm{cm}^{-3}$, $m_{\mathrm{RCA}} = -0.295\,\%\,\mathrm{cm}^{-3}$) while LCx scars led to an LVEF reduction of $-0.350\,\%$ per cm^3 of affected tissue.

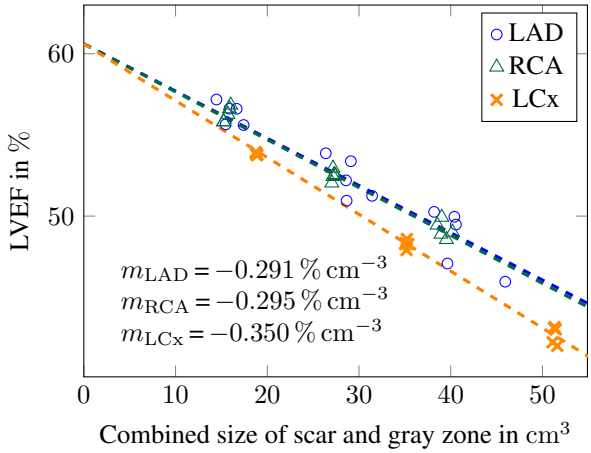

Figure 4. Relation of LVEF and affected myocardial volume (combined scar + gray zone) for the `Rodero-01` anatomy. Results are grouped according to their IRA (LAD: blue rings, RCA: green triangles, LCx: orange crosses).

4. Discussion and conclusion

We showed that at a given scar size, scar tissue in the left ventricular free wall (LCx-related scars) leads to more substantial reductions in LVEF than scar tissue in the septum. However, not only the size of the scar but also the size of the gray zone reduces LVEF. Automatic gray zone generation led to different sizes of total affected myocardial volume. Especially for LCx scars, this is apparent (see Fig. 4). Based on the reported values in [6], the maximum transmurality was approx. 100 % for LAD and RCA scars and 72 % for LCx scars. Since the LCx scars in this study are never fully transmural, the automatically generated gray zone extends also in transmural direction and consequently amounts to a larger total volume. With the choice of a constant $\eta = 0.1$ instead of a gradient for the gray zone following [13], the passive material behavior for the gray zone is similar to the one of scar tissue (refer to Equation 6), which in theory could be the sole reason behind the increased LVEF reduction in LCx scars. However, Figure 4 shows that this is not the case. For the same anatomy (`Rodero-01`), LVEF reduction is increased for LCx scars even if plotted over the combined volume of scar and gray zone. In fact, moderate LCx scars resulted in slightly lower LVEFs (mean LVEF: 48.28 %) compared to severe RCA and LAD scars (48.97 % and 48.55 %, respectively) while occupying less total myocardial volume (mean values: $35.18\,\mathrm{cm}^3$ compared to $39.24\,\mathrm{cm}^3$ and $40.95\,\mathrm{cm}^3$).

Our results indicate that not only the size but also the location of the scar tissue drives the reduction in LVEF for patients with CAD. Different slopes of the negative linear relation between scar (or scar + gray zone) size and LVEF for different scar locations is in agreement with clinical studies comparing myocardial infarct size and resulting LVEFs [15]. The existence of a threshold for which below a critical infarct size there is no change in LVEF as proposed by Pride et al. [15] (15 %) in 2010 and by Sciagrà et al. [16] (8 %) in 2013 could not be verified with our model. All simulations, including the ones with approx. 6.5 % scar size, show a decline in LVEF as compared to the control simulation with no scar tissue.

The presence of a large scar, as determined by the Selvester QRS score, has been shown to be an independent predictor of ventricular arrhythmias in ICD recipients with untreated chronic total coronary occlusion [17]. Furthermore, Scott et al. [18] reported in a single-center pilot study of patients with CAD and ICDs that the extent of myocardial scar characterized by LGE-CMR is strongly associated with the occurrence of spontaneous ventricular arrhythmias, independent of LVEF. In their study, LVEF was not associated with the study end point (appropriate ICD therapy). Similarly, Bello et al. [19] reported that infarct surface area and mass, as measured by cardiac MRI, are better identifiers for patients who have a substrate for monomorphic ventricular tachycardia than LVEF. In a recent study including more than 1000 patients suffering from non-ischemic cardiomyopathy, Klem et al. [5] re-

ported scar size to have strong prognostic value for SCD, but found no significant association between LVEF $\leq 35\,\%$ and SCD risk.

Combined with the results of this computational study, showing that similar scar sizes can lead to substantially different LVEFs, we believe that future clinical studies should include scar size estimation and focus less on LVEF.

Acknowledgments

This research was funded by Deutsche Forschungsgemeinschaft (DFG, German Research Foundation) - project #465189069 (LO 2093/6-2, SPP 2311) and #258734477 (SFB 1173). This work was performed on the computational resource bwUniCluster funded by the Ministry of Science, Research and the Arts Baden-Württemberg and the Universities of the State of Baden-Württemberg, Germany, within the framework program bwHPC.

References

[1] Kwon DH, Halley CM, Carrigan TP, et al. Extent of left ventricular scar predicts outcomes in ischemic cardiomyopathy patients with significantly reduced systolic function: A delayed hyperenhancement cardiac magnetic resonance study. JACC Cardiovasc Imaging 2009;2(1):34–44. ISSN 1936-878X.

[2] Halliday BP, Senior R, Pennell DJ. Assessing left ventricular systolic function: from ejection fraction to strain analysis. Eur Heart J 09 2020;42(7):789–797.

[3] Glikson M, Nielsen JC, Kronborg MB, et al. 2021 esc guidelines on cardiac pacing and cardiac resynchronization therapy: Developed by the task force on cardiac pacing and cardiac resynchronization therapy of the european society of cardiology (esc) with the special contribution of the european heart rhythm association (ehra). Eur Heart J 08 2021; 42(35):3427–3520.

[4] Russo AM, Desai MY, Do MM, et al. ACC/AHA/ASE/HFSA/HRS/SCAI/SCCT/SCMR 2025 appropriate use criteria for implantable cardioverter-defibrillators, cardiac resynchronization therapy, and pacing. J Am Coll Cardiol 2025;85(11):1213–1285.

[5] Klem I, Klein M, Khan M, et al. Relationship of LVEF and myocardial scar to long-term mortality risk and mode of death in patients with nonischemic cardiomyopathy. Circulation 2021;143(14):1343–1358.

[6] Woie L, Engan K, Eftestøl T, et al. The localization and characterization of ischemic scars in relation to the infarct related coronary artery assessed by cardiac magnetic resonance and a novel automatic postprocessing method. Cardiol Res Pract 1 2015;2015:1–9.

[7] Gerach T, Loewe A. Differential effects of mechano-electric feedback mechanisms on whole-heart activation, repolarization, and tension. J Physiol 2024;602(18):4605–4624.

[8] Gerach T, Schuler S, Wachter A, et al. Four-chamber human heart model for the simulation of cardiac electrophysiology and cardiac mechanics, January 2024. URL doi.org/10.5281/zenodo.10526554.

[9] Rodero C, Strocchi M, Marciniak M, et al. Virtual cohort of adult healthy four-chamber heart meshes from CT images, March 2021. URL doi.org/10.5281/zenodo.4590294.

[10] Azzolin L, Eichenlaub M, Nagel C, et al. Augmenta: Patient-specific augmented atrial model generation tool. Comput Med Imaging Graphics 2023;108:102265.

[11] Krauß J, Gerach T, Loewe A. Comparison of pericardium modeling approaches for mechanical whole heart simulations. In 2023 Computing in Cardiology (CinC), volume 50. IEEE, 2023; 1–4.

[12] Ten Tusscher KH, Panfilov AV. Alternans and spiral breakup in a human ventricular tissue model. Am J Physiol Heart Circ Physiol 2006;291(3):H1088–H1100.

[13] Salvador M, Fedele M, Africa PC, et al. Electromechanical modeling of human ventricles with ischemic cardiomyopathy: numerical simulations in sinus rhythm and under arrhythmia. Comp Biol Med 9 2021;136:104674.

[14] Arevalo HJ, Vadakkumpadan F, Guallar E, et al. Arrhythmia risk stratification of patients after myocardial infarction using personalized heart models. Nat Commun 2016; 7(1):11437.

[15] Pride YB, Giuseffi JL, Mohanavelu S, et al. Relation between infarct size in st-segment elevation myocardial infarction treated successfully by percutaneous coronary intervention and left ventricular ejection fraction three months after the infarct. Am J Cardiol 2010;106(5):635–640.

[16] Sciagrà R, Cipollini F, Berti V, et al. Detection of infarct size safety threshold for left ventricular ejection fraction impairment in acute myocardial infarction successfully treated with primary percutaneous coronary intervention. Eur J Nucl Med Mol Imaging 2013;40:542–547.

[17] Assaf A, van der Graaf M, van Boven N, et al. Effect of myocardial scar size on the risk of ventricular arrhythmias in patients with chronic total coronary occlusion. Int J Cardiol 11 2023;390:131205.

[18] Scott PA, Morgan JM, Carroll N, et al. The extent of left ventricular scar quantified by late gadolinium enhancement mri is associated with spontaneous ventricular arrhythmias in patients with coronary artery disease and implantable cardioverter-defibrillators. Circ Arrhythmia and Electrophysiol 6 2011;4(3):324–330.

[19] Bello D, Fieno DS, Kim RJ, et al. Infarct morphology identifies patients with substrate for sustained ventricular tachycardia. J Am Coll Cardiol 2005;45(7):1104–1108.

Address for correspondence:

Jonathan Krauß, publications@ibt.kit.edu
Institute of Biomedical Engineering, Karlsruhe Institute of Technology (KIT), Kaiserstr. 12, 76131, Karlsruhe, Germany.